Geophysical Research Letters

RESEARCH LETTER
10.1029/2020GL091496

Where Are Global Vegetation Greening and Browning Trends Significant?

José Cortés[1,2], Miguel D. Mahecha[2,3,4], Markus Reichstein[2], Ranga B. Myneni[5], Chi Chen[5], and Alexander Brenning[1]

[1]Department of Geography, Friedrich Schiller University, Jena, Germany, [2]Max Planck Institute for Biogeochemistry, Jena, Germany, [3]Remote Sensing Centre for Earth System Research, Leipzig University, Leipzig, Germany, [4]Remote Sensing Centre for Earth System Research, Helmholtz-Centre for Environmental Research, Leipzig, Germany, [5]Department of Earth and Environment, Boston University, Boston, MA, USA

Abstract Global greening trends have been widely reported based on long-term remote sensing data of terrestrial ecosystems. Typically, a hypothesis test is performed for each grid cell; this leads to multiple hypothesis testing and false positive trend detection. We reanalyze global greening and account for this issue with a novel statistical method that allows robust inference on greening regions. Based on leaf area index (LAI) data, our methods reduce the detected greening from 35.2% to 15.3% of the terrestrial land surface; this reduction is most notable in nonwoody vegetation. Our results confirm several greening regions (China, India, Europe, Sahel, North America, Brazil, and Siberia), that are also supported by independent data products. We also report evidence for an increasing seasonal amplitude in LAI north of 35°N. Considering the widespread use of spatially replicated trend tests in global change research, we recommend adopting the proposed multiple testing procedure to control false positive outcomes.

Plain Language Summary Using satellite data, recent studies have detected an increase in vegetation greenness around the globe. These studies attribute this vegetation increase to different factors, such as warming or land use change. However, we argue that the commonly used analysis method is detecting too many regions with trends. In this work, we reanalyze vegetation data using the leaf area index, which measures the area occupied by leaves in any given area. With our refined methods, we too detect greening regions around the world, however these regions are smaller and less abundant. Our research introduces a step in the statistical analysis that increases the reliability of the detected vegetation greening. This can help establish more consensus on what the main contributing factors are for the observed vegetation increase.

Key Points:

- Many studies have consistently reported on global greening trends, but repeatedly without rigorous significance testing
- Although global greening has been overestimated, significant greening can still be rigorously detected
- We observe an increase in the seasonal amplitude of leaf area index around the glob

Supporting Information:

- Supporting Information S1

Correspondence to:
J. Cortés,
jose.cortes@uni-jena.de

Citation:
Cortés, J., Mahecha, M. D., Reichstein, M., Myneni, R. B., Chen, C., & Brenning, A. (2021). Where are global vegetation greening and browning trends significant? *Geophysical Research Letters*, *48*, e2020GL091496. https://doi.org/10.1029/2020GL091496

Received 29 OCT 2020
Accepted 24 JAN 2021

Author Contributions:
Conceptualization: José Cortés, Miguel D. Mahecha, Markus Reichstein, Ranga B. Myneni, Chi Chen, Alexander Brenning
Formal analysis: José Cortés
Writing – original draft: José Cortés
Writing – review & editing: José Cortés, Miguel D. Mahecha, Markus Reichstein, Ranga B. Myneni, Chi Chen, Alexander Brenning

1. Introduction

The analysis of vegetation data based on satellite products has led to a consensus on a greening Earth. Changes in the terrestrial vegetation dynamics impact the Earth system (Intergovernmental Panel on Climate Change, 2014): changes in the Arctic tundra ecosystems can impact climate feedbacks as well as wildlife and human communities (Berner et al., 2020); an increase in greening could mean an increase in the land carbon sink (Ballantyne et al., 2012; J. M. Chen, Ju, et al., 2019; Piao et al., 2020); and global greening can mitigate increasing global land surface air temperatures (Feng & Zou, 2019; Z. Zeng et al., 2017). Therefore, determining the amount of greening and where it is occurring is essential. Today, there is much debate about the attribution of these greening trends to potential causes such as CO_2 fertilization, temperature rise, and land use intensification (C. Chen, Park, et al., 2019; Forzieri et al., 2017; Huang et al., 2017; Munier et al., 2018; Notaro et al., 2005; Yuan et al., 2019; Zhao et al., 2018; Zhu et al., 2016). A thorough review of the drivers of global greening can be found in Piao et al. (2020).

The common approach to quantify global greening is to analyze maps of statistically significant greening or browning trends, where any grid cell with a *p*-value under the nominal $\alpha = 0.05$ or $\alpha = 0.10$ is considered statistically significant (C. Chen, Park, et al., 2019; de Jong et al., 2012; Feng & Zou, 2019; Forzieri et al., 2017; Munier et al., 2018; Xiao & Moody, 2005; Yuan et al., 2019; Z. Zeng et al., 2017; Zhang et al., 2019; Zhao et al., 2018; Zhu et al., 2016). These grid cells are then used in a subsequent analysis, for example, for attribution analysis. However, here the issue of multiple hypothesis testing arises,

Table 1
The Five Data Products Used for Analysis And Comparison

Name	Variable(s)	Satellite	Domain and resolution	Reference
BU AVHRR LAI/GIMMS 3g V1	LAI	AVHRR	Global, 1/12°, bi-monthly, 1981–2018	Chen, Park, et al., 2019; Zhu et al., 2013
NOAA CDR	LAI	AVHRR	Global, 0.05°, daily, 1981–2019	Claverie et al., 2016
LTDR	LAI	AVHRR, MODIS	Global, 0.05°, daily, 1981–2018	Pedelty et al., 2007
BU MODIS C6	LAI	MOD15A2H; MYD15A2H	Global, 0.05°, 16 days, 2000–2019	C. Chen, Park, et al., 2019
SPOT/PROBA-V	LAI	MODIS, Cyclops	Global, 0.5°, 10 days, 1999–2018	Baret et al., 2013

BU AVHRR, Boston University Advanced Very-High-Resolution Radiometer; GIMMS, global inventory modeling and mapping studies; LAI, leaf area index; MODIS, moderate resolution imaging spectroradiometer; NOAA CDR, national oceanic and atmospheric administration's climate data record; LTDR, land long term data record.

potentially leading to inferred trends that are false positives: when performing hundreds of thousands of tests, which is the case of gridded datasets derived from satellite products - we expect $\alpha\%$ of all grid cells to be significant just by chance (false positives). Due to spatial autocorrelation, these false positives may lead to the interpretation of spurious spatial patterns. In the case of global greening and browning, previous studies have reported (at $\alpha = 0.10$) LAI trends in ~40% of the terrestrial land surface (~35% greening and ~5% browning). Therefore, we expect a fourth (0.10/0.40) of these trends to be false positives just due to the statistical testing mechanism.

The issue of multiple hypothesis testing has been raised in the environmental sciences, along with some common corrections for multiple hypothesis testing (Livezey & Chen, 1983; Ventura et al., 2004; Wilks, 2006, 2016), but these methods have not been widely adopted. We focus on a permutation method that allows us to make inference on regions of significant greening or browning, as shown recently by Cortés et al. (2020). This novel statistical method shall allow us to define clear focal areas of greening that can then be used in subsequent analysis.

In this work, we reanalyze global greening trends based on the Boston University Advanced Very-High-Resolution Radiometer (BU AVHRR) LAI data set and validate the results with four other data products: NOAA CDR, LTDR, BU moderate resolution imaging spectroradiometer (MODIS C6), and SPOT. We perform a Mann-Kendall (MK) trend test, which is a common significance test for the slope estimated by the Theil-Sen method. The latter is a nonparametric estimator of a linear trend, which tells us how the average LAI changes with time, but is robust against individual outliers. We correct all analyses for the multiplicity of hypothesis tests using a permutation method based on clustering. However, we also expect that the quantiles of LAI may behave differently than the mean over time. For example, an increase in the seasonal amplitude of LAI would make the 0.1 and 0.9 quantiles behave differently than the mean. To test this hypothesis, we also aggregate our yearly data into the 0.1, 0.25, 0.5, 0.75, and 0.9 quantiles, and perform trend tests on these quantiles.

The study is structured as follows. The five data products used in this study are further explained in Section 2. In Section 3, we detail our methodology. Our results and discussion are presented in Section 4, and we present our conclusions in Section 5.

2. Data

We analyze five data products that all aim at improving the estimates of Leaf Area Index (LAI) around the globe. These datasets are derived from different satellite products and use state of the art methodologies to ensure the quality and consistency of their estimates. Our results are based on the BU AVHRR LAI data, and validated with LAI data obtained from the National Oceanic and Atmospheric Administration's Climate Data Record (NOAA CDR), the Land long Term Data Record (LTDR), BU MODIS C6, and SPOT/PROBA-V. Further details can be found in Table 1.

3. Methods

Before applying the trend test, we aggregate the data into yearly values using several descriptive statistics: the mean, the 0.1, 0.25, 0.5, 0.75, and 0.9 quantiles, and the interdecile range (defined as the difference between the 0.90 and 0.10 quantiles). The ability to detect trends is not affected by this averaging, and the trend estimates are comparable to methods which use the unaveraged time series (Forkel et al., 2013). We use all available LAI values in the given year, as this is better suited for a global study and avoids issues such as defining a growing season, dealing with multiple growing seasons, and dealing with growing seasons that span two calendar years (C. Chen, Park, et al., 2019). We test for a trend with the nonparametric MK trend test (Kendall, 1975; Mann, 1945). The MK trend test is commonly used as a test of significance for the Theil-Sen estimator, which is a nonparametric method to estimate a monotonic trend from a time series.

Temporal autocorrelation is accounted for with an $AR(1)$correction. Not accounting for temporal autocorrelation can lead to increased false positive rates (von Storch, 1999). We follow the procedure outlined in von Storch (1999): for each grid cell, we calculate the temporal autocorrelation at lag-1, $\hat{r} = \frac{n \cdot \sum_1^{n-1}\left(\mathrm{x_i} - \overline{x}\right)\left(x_{i+1} - \overline{x}\right)}{\left(n-1\right) \cdot \sum_1^{n}\left(\mathrm{x_i} - \overline{x}\right)^2}$, and replace the original time-series, x_t, with the series $Y_t = x_t - \hat{r}x_{t-1}$. The MK trend test is then performed on this new time series. This procedure is applied to all of the data in this manuscript.

To correct for multiple hypothesis testing, we apply a permutation method based on clustering. The permutation test establishes a threshold for overall significance based on the number of contiguous (first-order queen neighbors) significant grid cells. The motivation behind this test is that the clusters formed by false positives are smaller than those formed where a true increase or decrease in vegetation exists. We perform 3,000 permutations to determine the threshold for significance. At each permutation, all grid cells are permuted jointly, that is, using the same set of permuted time indices. This preserves the spatial correlation of the data. The MK trend test is performed on this permuted data, and the largest cluster of significant grid cells is recorded. The $\left(1-\alpha\right)^{\mathrm{th}}$ quantile of the 3,000 recorded largest clusters is the threshold for overall significance. In our original data, for each significant region we count the number of grid cells, and if it exceeds the threshold established by the permutation method, we declare this region significant. This method has been proven to control the probability of having false positives in the results, and has higher statistical power than comparable methods, such as Bonferroni and related methods (Cortés et al., 2020).

For a consistent comparison of greening trends in different LAI products, we also analyze the time period from 2000 to 2018 for all data products.

4. Results and Discussion

We find consistent greening trends of the yearly LAI mean in the whole world: Asia (35% of overall global greening), Europe (32.5%), North America (13.3%), Africa (12.6%), South America (6%), and Australia (0.5%). These trends are detected mostly in the northern hemisphere (Figure 1). These greening patterns are consistent with those detected in other recent studies such as C. Chen, Park, et al. (2019); we detect the same greening patterns and, additionally, several more. Our results validate the main greening hotspots, but also suggest that other regions which have been discussed in other studies are not large enough to be statistically significant when analyzing the whole terrestrial land surface - for example, our study does not detect the greening and browning of Alaska (Berner et al., 2020; Forkel et al., 2013; Verbyla, 2008), the greening western Sahel zone (Dardel et al., 2014), and most of the greening of Australia (Ukkola et al., 2016). Our method assumes that false positive regions are smaller than true signal regions. It is reasonable to expect regions of greening to be much larger, due to the large scale global greening that has been reported. This is the case in our study, as evidenced by the detected greening across all continents. Nevertheless, there are still regions, as discussed previously, that are too small to be detected by our method when analyzing the whole world. Therefore, analyzing a smaller study region may reveal previously undetected trends.

We observe pockets of nonsignificant grid cells among the significant clusters. Because there is no wall-to-wall ground truth validation, noise in the trend can cause some small pockets. Larger pockets can be attrib-

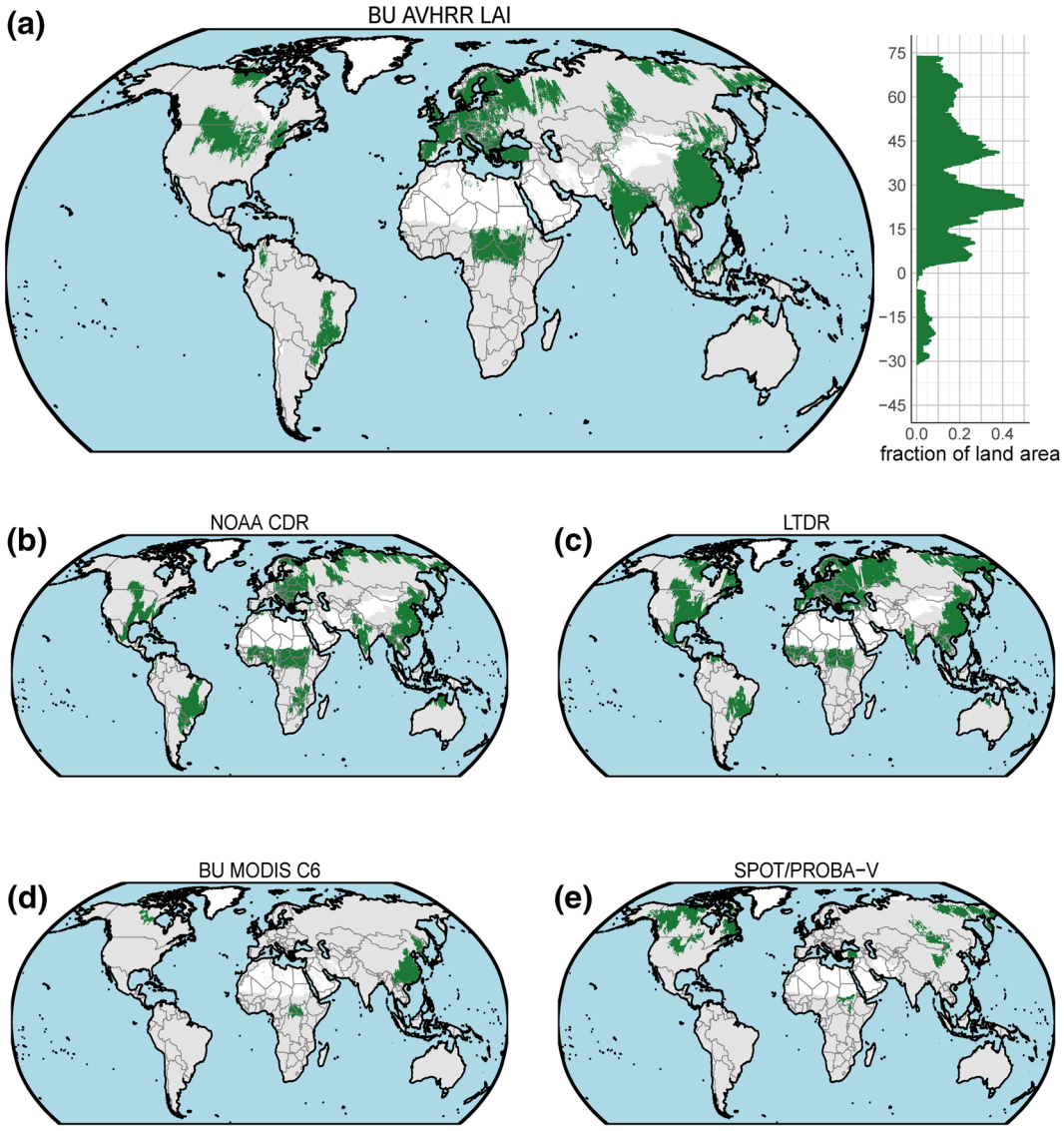

Figure 1. Significant LAI trends in each of the datasets, using the Mann-Kendall trend test, after correcting for multiple hypothesis testing. Green indicates a significant increasing trend at $\alpha = 0.10$. No browning is detected. Grid cells with no statistical significance are shown in gray. No hypothesis test performed for grid cells in white (barren land). Blue represents water. The distribution of significant greening by latitude is shown for BU AVHRR LAI. LAI, leaf area index.

uted to different biome types, caused by (sharp) elevation change in mountainous regions and different land use (e.g., urban vs. cropland).

We look only at monotonic trends for the whole period. Thus it is possible that there are strong piecewise trends (e.g., first greening, then browning) which lead to a nontrend overall. This has been observed by de Jong et al. (2012), who reported that 15% of the terrestrial land surface exhibits both greening and browning. The statistical testing of such trend changes, while taking into account the multiple hypothesis testing, will be an interesting follow-up study.

Not adjusting for multiple hypothesis testing can overestimate the global greening (Figure 2). After applying the correction, we detect greening in 15.3% of the terrestrial land surface, as opposed to 35.2% when no correction is applied. Similarly, greening within each continent can be three times larger or more when no correction for multiple testing is done. Particularly in Australia (26.1% reduced to 1%) and South America

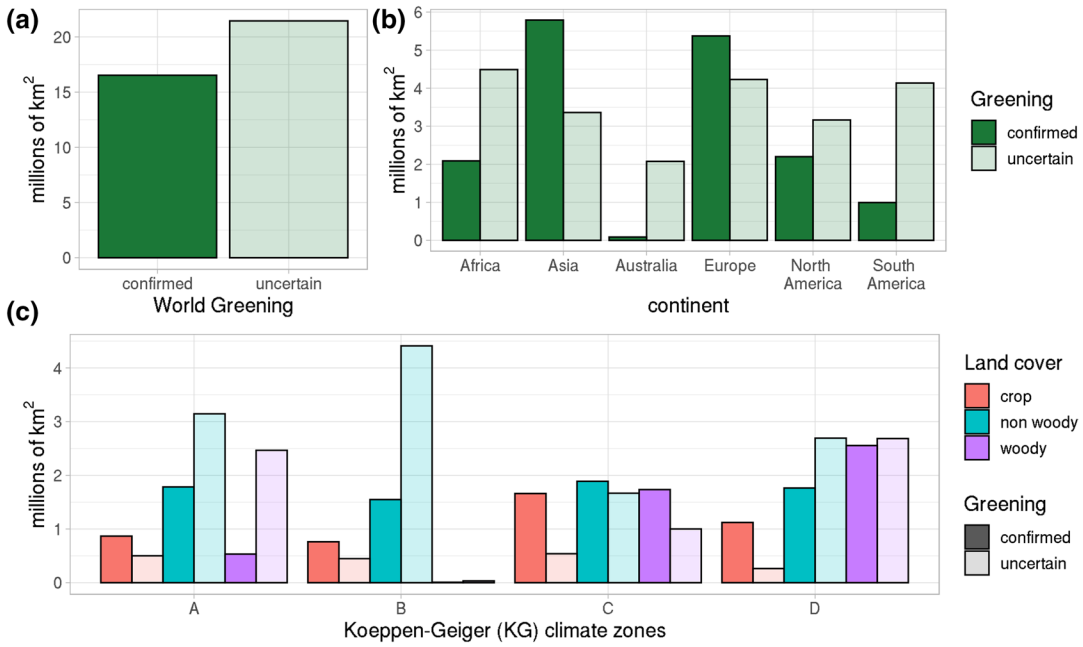

Figure 2. World greening, in millions of km^2, by (a) total land area, (b) continents, and (c) Koeppen-Geiger (KG) climate zones versus land cover type. Darker shades indicate greening that remains after correcting for multiple hypothesis testing ($\alpha = 0.10$), while lighter shades indicate the uncertain greening, that is, additional greening that is detected when no multiple testing correction is done. The KG climate zones are: A, Tropical; B, Dry; C, Temperate; and D, Continental. No browning withstands the correction for multiple hypothesis testing.

(26.7% reduced to 5.2%) we observe a great reduction in detected greening. We categorize areas as uncertain greening where there are grid cells whose trend signal is not strong enough to be detected by our method, but strong enough to be detected when performing no correction.

The discrepancy in the amount of overestimation by continent can be better understood by looking at the climate zones and land use type. This reveals that the uncertain greening occurs twice as much in non-woody compared to woody vegetation (Figure 2c), while there is very little uncertain greening in crop land. This is in line with previous studies that have observed prominent greening in cropland (de Jong et al., 2011; Piao et al., 2020). Piao et al. (2020) also observe strong greening in afforested regions and biomes with low human footprint, which coincides with the bulk of the confirmed greening that we detect in temperate and continental climate zones. The overestimation is particularly large in nonwoody vegetation within tropical and dry climate zones (Figure 2c). In tropical regions, large uncertainty is caused due to the saturation of LAI in dense vegetation, in addition to cloud and aerosol contaminants, while uncertainties in semi-arid climate and sparse vegetation can be due to the sensitivity of the vegetation indices to change in soil background (Piao et al., 2020).

Using the mean or the median to aggregate yearly values can impact the results. Both mean and median detect similar greening regions, but browning is only detected when using the median (Figure 3). While the mean detects greening in ~16.6 million km^2 (273,247 grid cells) of the land surface and no browning, the median detects greening in ~15.8 million km^2 (258,385 grid cells) and browning in 1.1 million km^2 (26,241 grid cells) of the land surface. Two browning patterns arise when using the yearly median: one in Siberia and one in Canada. Previous studies have indicated a reversal or stalled greening in high latitudes (Gonsamo et al., 2019), and it is argued that increased plant growth in spring and earlier start of the growing season leads to decreased summer growth and decreased peak season maximum plant growth. When correcting for multiple testing, the summarizing statistic should not be overlooked when analyzing global greening and browning trends. Previous studies commonly use the average, so a reanalysis using the median can potentially reveal new browning patterns and reduce greening regions.

The mean is not sufficient to describe the LAI trends over time, looking at quantiles reveals additional greening and browning trends. While the upper quantiles (0.75, 0.90) detect similar greening regions as

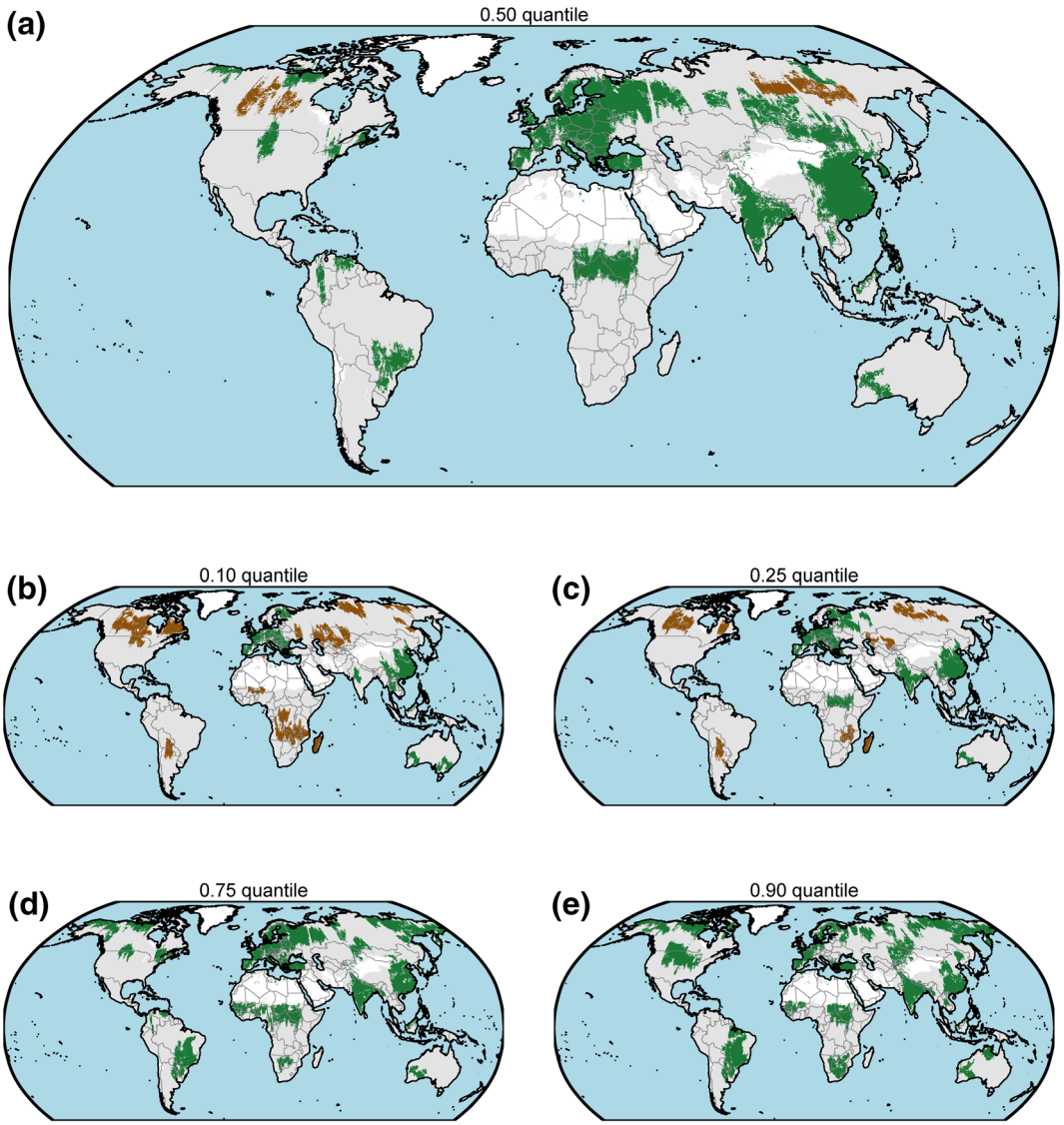

Figure 3. Significant LAI trends in the BU AVHRR LAI data set, after correcting for multiple hypothesis testing, using the (a) 0.50 quantile (median) and the yearly (b) 0.10, (c) 0.25, (d) 0.75, and (e) 0.90 quantiles. Green (brown) indicates a significant increasing (decreasing) trend at $\alpha = 0.10$. Grid cells with no statistical significance are shown in gray. No hypothesis test performed for grid cells in white (barren land). Blue represents water. LAI, leaf area index.

the mean and median, the lower quantiles (0.10, 0.25) reveal browning trends in specific regional clusters around the globe (Figure 3). When we look at the distribution of *Z*-scores obtained from the LAI trends throughout the quantiles, there is a shift from most grid cells indicating browning at the 0.10 quantile to most grid cells indicating greening at the 0.90 quantile (Figure S1). The bulk of the distribution shifts from browning to greening, which hints toward an increase in the seasonal amplitude around the globe. We further investigate this by analyzing the interdecile range, which shows the regions where we detect several regions of significant increase in the seasonal amplitude of LAI (Figure S1). An increase in seasonal amplitude has been previously observed and could be due to trends in deforestation, fertilization and climate change effects, and/or changes in management (Kraemer et al., 2020).

The growing season in the higher latitudes has been expanding (Wolfe et al., 2005; H. Zeng et al., 2011; Ziska et al., 2011). This can cause the browning trends at the 0.10, 0.25, and 0.50 quantiles in the northern latitudes, since more low LAI values are detected each year. Previously these values were missing (marked as NA in the datasets), and they did not contribute toward the yearly aggregate. We would expect the trends

at the 0.10 quantile to be the most affected, yet most of these are validated by being detected at the 0.25 quantile. Unlike the median, the mean does not detect browning when analyzing yearly trends. This can be explained by the increase in peak summer vegetation which, as opposed to the longer growing season, is driving the greening trends in Eurasian boreal forests (Gao et al., 2020). The mean is more affected than the median by these summer peaks and therefore does not detect browning.

A large increase in the seasonal amplitude of CO_2 (at least 50%) has also been observed at all latitudes north of 45°N, and to a lesser extent (~26%) between 35°N and 45°N (Graven et al., 2013). It is argued that this increase can be caused by the ecosystems growing and shrinking more than before. These ecological changes are corroborated by the increasing and decreasing vegetation trends found previously in the northern hemisphere (Myneni et al., 1997), which we confirm with our rigorous significance testing. Furthermore, the regions where we detect an increase in the seasonal amplitude of LAI are also concentrated north of 35°N.

When considering a comparable time span (2000–2018), there is no longer such consistency (Figure S2). Few regions are detected by more than one data product, e.g., greening in southeast China is only detected by BU AVHRR LAI and BU MODIS C6, and greening in northern Canada is only detected by BU MODIS C6 and SPOT/PROBA V. In contrast to all other datasets, the LTDR detects browning in the Amazon forest, central Africa, Madagascar, and India. These results can be caused by several effects. For example, when shortening the time span, there may no longer be enough evidence to detect many greening trends. To explore this hypothesis, we test all possible 19 year periods in the BU AVHRR LAI data, that is, we analyzed the trends from 1981 to 2000, 1982 to 2001, ..., 2000 to2018. Only for 4 (out of 20) of these time periods we found few additional greening trends in the Sahel region (Figure S3). We find this still inconclusive – it is possible that the trends are missing due to a combination of (a) not enough data points and (b) a change in trend within the time series. Related to (b), abrupt and gradual changes in trend have been observed in large parts of the world by de Jone et al. (2012). A change in trend can also explain the browning found in the LTDR (e.g., greening from 1981 to 2000 can mask the browning from 2000 to 2018). The ability to detect a yearly trend is affected by this shortening.

All datasets that go back to 1981, BU AVHRR LAI, NOAA CDR, and LTDR, agree on the greening regions found in Europe, China, India, North America, Brazil, the Sahel, and Siberia. Thus we have more confidence in these observed greening patterns. Investigating these regions further with trend-attribution methods is an opportunity for further research.

In this work, we have introduced a new step, correcting for multiple hypothesis testing, when analyzing global LAI trends. However, the principles are very generic and relevant to most of the spatiotemporal dynamics encoded today in the growing global multivariate Earth system data cubes (Mahecha et al., 2020). For all these data streams, the presented methodology offers a quantitative way to automatically detect regions of statistically significant trends in either direction while controlling the probability of detecting false positives. By controlling the probability of detecting false positives, we make the detected trends more robust.

5. Conclusions

Many studies confirm that the Earth is greening but can differ in their explanation. We argue that a key step for analyzing the greening trends is missing - in our study we have introduced and applied a novel method that is often overlooked in a statistical analysis: a multiple hypothesis testing correction. In this work we apply a permutation-based correction to LAI trends and analyze yearly trends of the mean and the 0.10, 0.25, 0.50, 0.75, and 0.90 quantiles.

We detect greening in 15% of the terrestrial land surface, as opposed to 35% when applying no multiple testing correction. Still, we detect several hotspots that now stand out more prominently and consistently across the five data products that were analyzed. This overestimation happens twice as much in nonwoody vegetation than woody vegetation, and particularly in tropical and dry climate zones. Greening detected in crop land is the most reliable. Browning is only detected when aggregating the yearly data using the median instead of the mean. Additionally, we observe an increase in the seasonal amplitude of LAI around the globe.

Data Availability Statement

The NOAA Climate Data Record of Leaf Area Index available from https://data.nodc.noaa.gov/cgi-bin/iso?id=gov.noaa.ncdc:C00898. The Land Long Term Data Record (LTDR) available from https://ltdr.modaps.eosdis.nasa.gov/cgi-bin/ltdr/ltdrPage.cgi. The SPOT/PROBA-V data available from https://icdc.cen.uni-hamburg.de/lai-spot-probav.html.

Acknowledgments
The authors would like to thank the following institutions for generously providing the data used in this study: the National Oceanic and Atmospheric Administration (NOAA), which provides the NOAA Climate Data Record of Leaf Area Index available from https://data.nodc.noaa.gov/cgi-bin/iso?id=gov.noaa.ncdc:C00898; NASA's Goddard Space Flight Center, which provides the Land Long Term Data Record (LTDR) available from https://ltdr.modaps.eosdis.nasa.gov/cgi-bin/ltdr/ltdrPage.cgi; and the Integrated Climate Data Center (ICDC), which provides the SPOT/PROBA-V data available from https://icdc.cen.uni-hamburg.de/lai-spot-probav.html. The authors would also like to acknowledge the work of Ulrich Weber at the Max-Planck-Institute for Biogeochemistry and Stefan Kern at the ICDC for the data curation. R. B. Myneni thanks NASA Earth Science Division for funding his participation in this research. J. Cortés is supported by the Free State of Thuringia through a graduate student scholarship and acknowledges support by the International Max Planck Research School for Global Biogeochemical Cycles (IMPRS-gBGC).

References

Ballantyne, A. P., Alden, C. B., Miller, J. B., Tans, P. P., & White, J. W. C. (2012). Increase in observed net carbon dioxide uptake by land and oceans during the past 50 years. *Nature*, *488*(7409), 70–72. https://doi.org/10.1038/nature11299

Baret, F., Weiss, M., Lacaze, R., Camacho, F., Makhmara, H., Pacholcyzk, P., & Smets, B. (2013). GEOV1: LAI and FAPAR essential climate variables and FCOVER global time series capitalizing over existing products. Part 1: Principles of development and production. *Remote Sensing of Environment*, *137*, 299–309. https://doi.org/10.1016/j.rse.2012.12.027

Berner, L. T., Massey, R., Jantz, P., Forbes, B. C., Macias-Fauria, M., Myers-Smith, I., et al. (2020). Summer warming explains widespread but not uniform greening in the Arctic tundra biome. *Nature Communications*, *11*(1), 4621. https://doi.org/10.1038/s41467-020-18479-5

Chen, C., Park, T., Wang, X., Piao, S., Xu, B., Chaturvedi, R. K., et al. (2019a). China and India lead in greening of the world through land-use management. *Nature Sustainability*, *2*(2), 122–129. https://doi.org/10.1038/s41893-019-0220-7

Chen, J. M., Ju, W., Ciais, P., Viovy, N., Liu, R., Liu, Y., & Lu, X. (2019b). Vegetation structural change since 1981 significantly enhanced the terrestrial carbon sink. *Nature Communications*, *10*(1), 4259. https://doi.org/10.1038/s41467-019-12257-8

Claverie, M., Matthews, J., Vermote, E., & Justice, C. (2016). A 30+ year AVHRR LAI and FAPAR climate data record: algorithm description and validation. *Remote Sensing*, *8*(3), 263. https://doi.org/10.3390/rs8030263

Cortés, J., Mahecha, M., Reichstein, M., & Brenning, A. (2020). Accounting for multiple testing in the analysis of spatio-temporal environmental data. *Environmental and Ecological Statistics*, *27*(2), 293–318. https://doi.org/10.1007/s10651-020-00446-4

Dardel, C., Kergoat, L., Hiernaux, P., Mougin, E., Grippa, M., & Tucker, C. J. (2014). Re-greening Sahel: 30 years of remote sensing data and field observations (Mali, Niger). *Remote Sensing of Environment*, *140*, 350–364. https://doi.org/10.1016/j.rse.2013.09.011

de Jong, R., de Bruin, S., de Wit, A., Schaepman, M. E., & Dent, D. L. (2011). Analysis of monotonic greening and browning trends from global NDVI time-series. *Remote Sensing of Environment*, *115*(2), 692–702. https://doi.org/10.1016/j.rse.2010.10.011

de Jong, R., Verbesselt, J., Schaepman, M. E., & Bruin, S. (2012). Trend changes in global greening and browning: Contribution of short-term trends to longer-term change. *Global Change Biology*, *18*(2), 642–655. https://doi.org/10.1111/j.1365-2486.2011.02578.x

Feng, H., & Zou, B. (2019). A greening world enhances the surface-air temperature difference. *Science of the Total Environment*, *658*, 385–394. https://doi.org/10.1016/j.scitotenv.2018.12.210

Forkel, M., Carvalhais, N., Verbesselt, J., Mahecha, M., Neigh, C., & Reichstein, M. (2013). Trend change detection in NDVI time series: Effects of inter-annual variability and methodology. *Remote Sensing*, *5*(5), 2113–2144. https://doi.org/10.3390/rs5052113

Forzieri, G., Alkama, R., Miralles, D. G., & Cescatti, A. (2017). Satellites reveal contrasting responses of regional climate to the widespread greening of Earth. *Science*, *356*(6343), 1180–1184. https://doi.org/10.1126/science.aal1727

Gao, X., Liang, S., & Sauer, J. (2020). Greening hiatus in Eurasian boreal forests since 1997 caused by a wetting and cooling summer climate. *Journal of Geophysical Research: Biogeosciences*, *125*(9), e2020JG005662. https://doi.org/10.1029/2020JG005662

Gonsamo, A., Ter-Mikaelian, M. T., Chen, J. M., & Chen, J. (2019). Does earlier and increased spring plant growth lead to reduced summer soil moisture and plant growth on landscapes typical of tundra-taiga interface? *Remote Sensing*, *11*(17), 1989. https://doi.org/10.3390/rs11171989

Graven, H. D., Keeling, R. F., Piper, S. C., Patra, P. K., Stephens, B. B., Wofsy, S. C., et al. (2013). Enhanced seasonal exchange of CO2 by northern ecosystems since 1960. *Science*, *341*(6150), 1085–1089. https://doi.org/10.1126/science.1239207

Huang, M., Piao, S., Janssens, I. A., Zhu, Z., Wang, T., Wu, D., et al. (2017). Velocity of change in vegetation productivity over northern high latitudes. *Nature Ecology and Evolution*, *1*(11), 1649–1654. https://doi.org/10.1038/s41559-017-0328-y

Intergovernmental Panel on Climate Change. (2014). *Climate change 2013: The physical science basis: Working Group I contribution to the Fifth Assessment Report of the Intergovernmental Panel on Climate Change*. In T. F. Stocker, D. Qin, G.-K. Plattner, M. Tignor, S. K. Allen, J. Boschung, et al. (Eds.), Cambridge University Press. https://doi.org/10.1017/CBO9781107415324

Kendall, M. G. (1975). *Rank correlation methods* (p. 160). New York, NY: Oxford University Press.

Kraemer, G., Camps-Valls, G., Reichstein, M., & Mahecha, M. D. (2020). Summarizing the state of the terrestrial biosphere in few dimensions. *Biogeosciences*, *17*(9), 2397–2424. https://doi.org/10.5194/bg-17-2397-2020

Livezey, R. E., & Chen, W. Y. (1983). Statistical field significance and its determination by Monte Carlo techniques. *Monthly Weather Review*, *111*(1), 46–59. https://doi.org/10.1175/1520-0493(1983)111<0046:SFSAID>2.0.CO;2

Mahecha, M. D., Gans, F., Brandt, G., Christiansen, R., Cornell, S. E., Fomferra, N., et al. (2020). Earth system data cubes unravel global multivariate dynamics. *Earth System Dynamics*, *11*(1), 201–234. https://doi.org/10.5194/esd-11-201-2020

Mann, H. B. (1945). Nonparametric tests against trend. *Econometrica*, *13*(3), 245–259. https://doi.org/10.2307/1907187

Munier, S., Carrer, D., Planque, C., Camacho, F., Albergel, C., & Calvet, J.-C. (2018). Satellite leaf area index: Global scale analysis of the tendencies per vegetation type over the last 17 years. *Remote Sensing*, *10*(3), 424. https://doi.org/10.3390/rs10030424

Myneni, R. B., Keeling, C. D., Tucker, C. J., Asrar, G., & Nemani, R. R. (1997). Increased plant growth in the northern high latitudes from 1981 to 1991. *Nature*, *386*(6626), 698–702. https://doi.org/10.1038/386698a0

Notaro, M., Liu, Z., Gallimore, R., Vavrus, S. J., Kutzbach, J. E., Prentice, I. C., & Jacob, R. L. (2005). Simulated and observed preindustrial to modern vegetation and climate changes*. *Journal of Climate*, *18*(17), 3650–3671. https://doi.org/10.1175/JCLI3501.1

Pedelty, J., Devadiga, S., Masouka, E., Brown, M., Pinzon, J., Tucker, C., et al. (2007). Generating a long-term land data record from the AVHRR and MODIS instruments. *International geoscience and remote sensing symposium*, 1021–1025. https://doi.org/10.1109/IGARSS.2007.4422974

Piao, S., Wang, X., Park, T., Chen, C., Lian, X., He, Y., et al. (2020). Characteristics, drivers and feedbacks of global greening. *Nature Reviews Earth & Environment*, *1*(1), 14–27. https://doi.org/10.1038/s43017-019-0001-x

Ukkola, A. M., Prentice, I. C., Keenan, T. F., van Dijk, A. I. J. M., Viney, N. R., Myneni, R. B., & Bi, J. (2016). Reduced streamflow in water-stressed climates consistent with CO2 effects on vegetation. *Nature Climate Change*, *6*(1), 75–78. https://doi.org/10.1038/nclimate2831

Ventura, V., Paciorek, C. J., & Risbey, J. S. (2004). Controlling the proportion of falsely rejected hypotheses when conducting multiple tests with climatological data. *Journal of Climate*, *17*(22), 4343–4356. https://doi.org/10.1175/3199.1

Verbyla, D. (2008). The greening and browning of Alaska based on 1982–2003 satellite data. *Global Ecology and Biogeography*, *17*(4), 547–555. https://doi.org/10.1111/j.1466-8238.2008.00396.x

von Storch, H (1999). Misuses of statistical analysis in climate research. In von Storch, H., & Navarra, A. (Eds.), *Analysis of climate variability* (pp. 11–26). Berlin, BE: Springer. https://doi.org/10.1007/978-3-662-03744-7_2

Wilks, D. S. (2006). On "field significance" and the false discovery rate. *Journal of Applied Meteorology and Climatology*, *45*(9), 1181–1189. https://doi.org/10.1175/JAM2404.1

Wilks, D. S. (2016). "The stippling shows statistically significant grid points": How research results are routinely overstated and overinterpreted, and what to do about it. *Bulletin of the American Meteorological Society*, *97*(12), 2263–2273. https://doi.org/10.1175/BAMS-D-15-00267.1

Wolfe, D. W., Schwartz, M. D., Lakso, A. N., Otsuki, Y., Pool, R. M., & Shaulis, N. J. (2005). Climate change and shifts in spring phenology of three horticultural woody perennials in northeastern USA. *International Journal of Biometeorology*, *49*(5), 303–309. https://doi.org/10.1007/s00484-004-0248-9

Xiao, J., & Moody, A. (2005). Geographical distribution of global greening trends and their climatic correlates: 1982–1998. *International Journal of Remote Sensing*, *26*(11), 2371–2390. https://doi.org/10.1080/01431160500033682

Yuan, W., Zheng, Y., Piao, S., Ciais, P., Lombardozzi, D., Wang, Y., et al. (2019). Increased atmospheric vapor pressure deficit reduces global vegetation growth. *Science Advances*, *5*(8), eaax1396. https://doi.org/10.1126/sciadv.aax1396

Zeng, H., Jia, G., & Epstein, H. (2011). Recent changes in phenology over the northern high latitudes detected from multi-satellite data. *Environmental Research Letters*, *6*(4), 045508. https://doi.org/10.1088/1748-9326/6/4/045508

Zeng, Z., Piao, S., Li, L. Z. X., Zhou, L., Ciais, P., Wang, T., et al. (2017). Climate mitigation from vegetation biophysical feedbacks during the past three decades. *Nature Climate Change*, *7*(6), 432–436. https://doi.org/10.1038/nclimate3299

Zhang, Y., Song, C., Band, L. E., & Sun, G. (2019). No proportional increase of terrestrial gross carbon sequestration from the greening Earth. *Journal of Geophysical Research: Biogeosciences*, *124*(8), 2540–2553. https://doi.org/10.1029/2018JG004917

Zhao, L., Dai, A., & Dong, B. (2018). Changes in global vegetation activity and its driving factors during 1982–2013. *Agricultural and Forest Meteorology*, *249*, 198–209. https://doi.org/10.1016/j.agrformet.2017.11.013

Zhu, Z., Bi, J., Pan, Y., Ganguly, S., Anav, A., Xu, L., et al. (2013). Global data sets of vegetation leaf area index (LAI)3g and fraction of photosynthetically active radiation (FPAR)3g derived from global inventory modeling and mapping studies (GIMMS) normalized difference vegetation index (NDVI3g) for the period 1981 to 2011. *Remote Sensing*, *5*(2), 927–948. https://doi.org/10.3390/rs5020927

Zhu, Z., Piao, S., Myneni, R. B., Huang, M., Zeng, Z., Canadell, J. G., et al. (2016). Greening of the Earth and its drivers. *Nature Climate Change*, *6*(8), 791–795. https://doi.org/10.1038/nclimate3004

Ziska, L., Knowlton, K., Rogers, C., Dalan, D., Tierney, N., Elder, M. A., et al. (2011). Recent warming by latitude associated with increased length of ragweed pollen season in central North America. *Proceedings of the National Academy of Sciences*, *108*(10), 4248–4251. https://doi.org/10.1073/pnas.1014107108